

H. S. Köhler ¹

Physics Department, University of Arizona, Tucson, Arizona 85721, USA

Abstract

This report concerns the energy of neutron-matter for densities below $0.15 fm^{-3}$ and temperatures at and below $10 MeV$. Separable NN-interactions are obtained by inverse scattering from the experimental phase-shifts with specified momentum cut-offs Λ . Results of Brueckner-Bloch-DeDomicis as well as finite temperature Green's function calculations show independence of cut-off for $\Lambda \geq 3$. Agreement with the low-density virial expansion is found. Results of Hartree-Fock as well as second order calculations show considerable Λ -dependence and the agreement with the virial expansion is lost. The "best" first-order choice of Λ is found to be $\sim 2.5 fm^{-1}$, which agrees with $V_{low k}$ studies. Reasonable agreement between the second order and the Brueckner results is also found for this value of Λ except at low density. Only 2-body forces are used in this study.

1 Introduction

The equation of state (EOS) of neutron matter is of particular interest in astrophysical studies. The mass of neutron-stars is related to the EOS at high density $\sim 0.5 - 0.7 fm^{-3}$. Lower densities $\leq 0.15 fm^{-3}$ are however of interest in problems related to supernova explosions. The zero temperature Brueckner theory is a well tested method at such densities. A finite temperature extension of this theory was given by Bloch and De Domicis.[1] It is used here and comparisons are made with the finite temperature Green's function method. A main difference from the Brueckner method is that the latter includes the spectral broadening self-consistently and the consequences of this broadening has to be investigated. Also, the spectral function contains all one-body properties. In that sense it supersedes the Brueckner method. It connects seamlessly to the non-equilibrium Green's function quantum transport theory being the stationary solution of this time-dependent theory. The spectral functions approach a quasi-particle (Brueckner) limit at low temperatures and low density and the energy-integrations that are part of the Green's function method then become numerically difficult. The Green's function method is therefore used only at high density and temperature and comparison with the Brueckner-Bloch-DeDomicis method shows satisfactory agreement here.

There are numerous publications related to the energy of a low density neutron gas, mostly at zero temperature. The results in one of the earliest[2] already agree satisfactorily with the most recent[3, 4, 5] at densities low enough for the 1S_0 -state to be dominant, even though the methods have been different. The finite temperature equation of state has been studied in detailed calculations by Margueron et al[6] and by Baldo et al[9] using Bloch-De Domicis methods. It is the focus of the present work. Our study also relates to recent works by Tolos et al[4] using Kohn-Luttinger-Ward methods, and by Horowitz and Schwenk[10]. A main purpose of the present study is to illustrate the usefulness of separable interactions that are directly related to scattering phase-shifts by inverse scattering to investigate the dependence on cut-offs in momentum-space. The study should be considered as exploratory. Any "final" precision calculation of nuclear properties should be based on 2- 3- (and many-body) forces derived from first principles.

The potentials are fitted to on-shell scattering data and the ranks of the potentials are the minimum required for these fits. If off-shell data are available these can also be fitted by increasing the rank. These data could in principle come directly from experiments or from meson-theoretical potentials. In case of the $^3S_1 - ^3D_1$ -states the deuteron provides such off-shell information. This was used in ref[11]. For the problem at hand, neutron-matter, this is not relevant. Here the main state is the 1S_0 . For reasons stated below this state is expected to be a good candidate for a separable interaction. It was indeed found in ref[11] that the half-off shell reactance matrix elements reproduced the Bonn-B potential data.

The basic equations used for the inverse scattering problem, the effective interaction in Brueckner theory (the G-matrix) and the role of the momentum cut-off is presented in Section 2. A short summary of the Green's function method with its effective interaction (the in-medium T-matrix) is given in Section 3. Section 4 presents the results of the numerical calculations while a summary of the findings is found in Section 5.

¹e-mail: kohler@physics.arizona.edu

2 Separable NN-interaction and Brueckner Theory

Because the S -states have poles near $E = 0$ a reasonable ansatz is to assume that these potentials are separable.[12] The inverse scattering method allows the numerical construction of a separable potential that reproduces a given set of phase-shifts EXACTLY. This method was used in ref. [11] with application to the energy of symmetric nuclear matter. The agreement with Bonn-B results was particularly impressive for the 1S_0 -state but also showed surprising agreement for all states except the 3P_1 for which it was found that the half-shell reactance matrix differed substantially. The Arndt phases[13] were used then and are also used here but at low energy supplemented by the phases obtained from the NN scattering length ($a_{nn} = -18.5 fm$) and effective range ($r_c = 2.68 fm$). The effect of low-momentum cut-offs was investigated in several subsequent papers [14, 15, 16, 17] and the connection with $V_{low k}$ was shown. (See for example Fig. 1 in ref. [17]). Readers are referred to these earlier publications for details regarding inverse scattering. Only a short summary and some important features of the method are shown below. A rank one separable potential is adequate at low density with low relative momenta between the nucleons. But the 1S_0 phases turn repulsive above $k_c \sim 1.6 fm^{-1}$ necessitating a rank 2 potential as a minimum requirement to fit these phase-shifts and others behaving similarly. Below are only presented the rank one formalism applicable for momentum cut-offs $\Lambda \leq k_c$. For larger cut-offs that require a rank 2 potential the equations are modified as in previous work [11] using the Bolsterli and MacKenzie method[18]. This is (of course) not a unique method of constructing a potential but as stated above it was found to give good agreement with the Bonn and presumably with other realistic potentials.[11]

For a rank one separable interaction one has, with the cut-off Λ indicated explicitly as a parameter

$$\langle k|V_\Lambda|p \rangle = -v(k; \Lambda)v(p; \Lambda) \quad (1)$$

From inverse scattering one finds:

$$v^2(k; \Lambda) = \frac{(4\pi)^2}{k} \sin\delta(k) |D(k^2)| \quad (2)$$

where

$$D(k^2) = \exp \left[\frac{2}{\pi} \mathcal{P} \int_0^\Lambda \frac{k' \delta(k')}{k^2 - k'^2} dk' \right] \quad (3)$$

where \mathcal{P} denotes the principal value and $\delta(k)$ is the scattering phase-shift.

Fig. 1 in ref.[16] shows results of Brueckner calculations with this potential in the $1S_0$ -state. There are two curves. The uppermost shows the potential energy as a function of Λ with dispersion-correction, the lower without this correction. The density is given by $k_f = 1.35 fm^{-1}$. The difference between the two curves is small. What is also important here is that the energy is constant for $\Lambda \geq \sim 2.5 fm^{-1}$. It is however equally important that this is a result of a ladder-summation to all orders, Brueckner theory.

The interaction obtained from the inverse scattering depends on the parameter Λ as shown already by Fig. 3 in ref.[17] so to first order in the interaction the energy is not expected to be independent of Λ . This is demonstrated in numerical examples below where the second and all order terms are also considered.

The Λ -dependence is further illustrated here by Fig. 1 showing $\langle k|V_\Lambda|k \rangle$ for two values of Λ . Although the two potentials are notably very different from each other they have in common that they both fit the phase-shifts EXACTLY for all $k < 2 fm^{-1}$. The $\Lambda = 8 fm^{-1}$ potential of course ALSO fits the phases from $2 \rightarrow 8 fm^{-1}$.

This means that the diagonal of the reactance matrix defined by

$$K(k) = -\frac{v^2(k; \Lambda)}{1 + I_K(k)} = -4\pi \cdot \tan\delta(k)/k \quad (4)$$

with

$$I_K(k) = \frac{1}{(2\pi)^3} \mathcal{P} \int_0^\Lambda \frac{v^2(k'; \Lambda)}{k^2 - k'^2} k'^2 dk' \quad (5)$$

is independent of Λ for $k \leq \Lambda$. Notice that eq. 4 implies a summation to all orders in V . The in-medium interaction defined by the Brueckner G -matrix (or by the in-medium T -matrix defined with Green's functions) differs from the reactance matrix K by the Pauli-blocking. Neglecting the dispersion-correction which in our case is small (see above), i.e. with no self-energy in the propagator, we have

$$G(k, P) = -\frac{v^2(k)}{1 + I_G(k, P)} \quad (6)$$

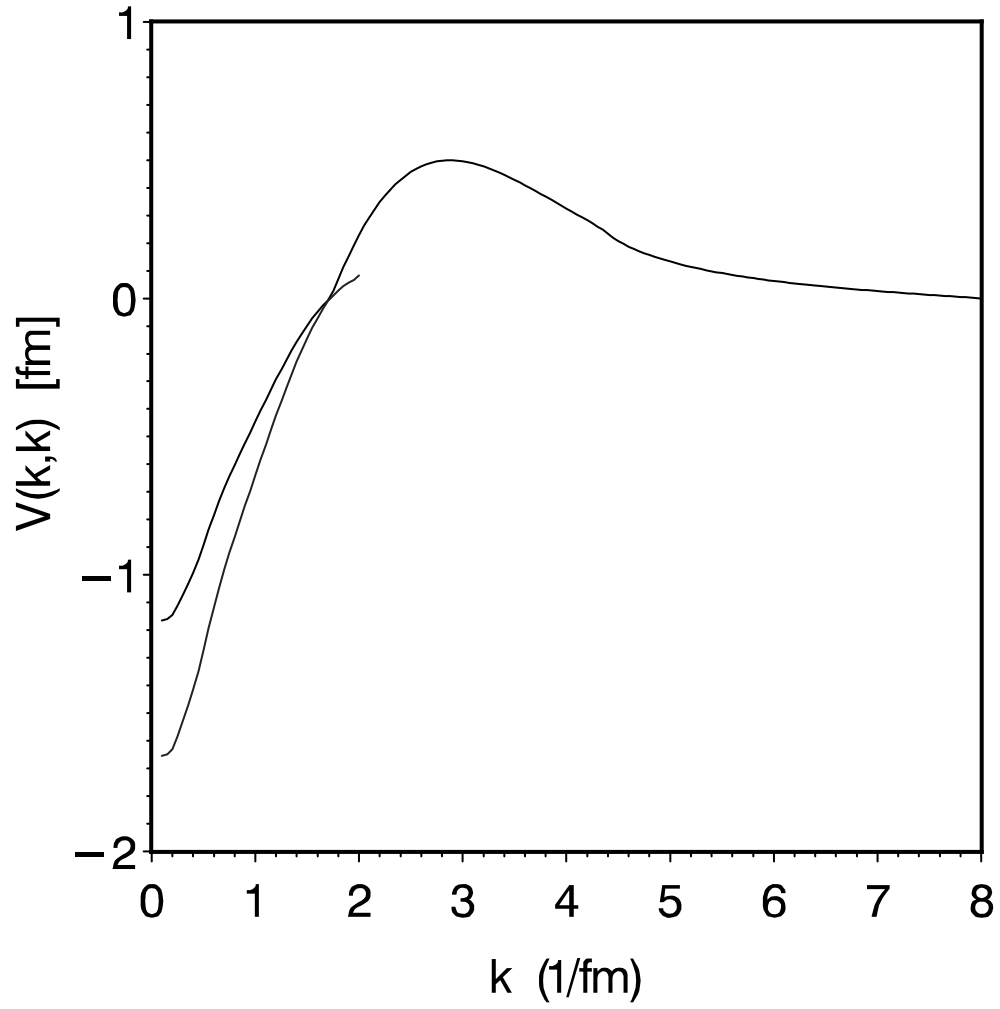


Figure 1: These curves illustrate the dependence of the 1S_0 -interaction on Λ as obtained from the inverse scattering. The maximum value of momentum for each of the two curves is at the two chosen values of Λ , 2 and 8fm^{-1} respectively.

with

$$I_G(k, P) = \frac{1}{(2\pi)^3} \int_0^\Lambda v^2(k') \frac{Q(k', P)}{k^2 - k'^2} k'^2 dk' \quad (7)$$

where P is the center of mass momentum and Q the angle-averaged Pauli-operator for pp-ladders, being exact with only kinetic energy in the denominator.

With the Pauli-blocking one has to expect G unlike K to be Λ -dependent. Calculations show however near independence even here as long as $\Lambda \geq 2k_f$. [16] This is exemplified by Fig. 2 showing G -matrix elements calculated from the two potentials of Fig. 1. The two curves overlap completely even though the potential are quite different. The center-of-mass momentum is here chosen to be zero, which gives the maximum effect of the Q -operator.

Further numerical investigations of the Λ -dependence as well as of ladder-expansions will be shown below. A few observations can be done without reference to detailed calculations. Let the density of nucleons $\rightarrow 0$. Then $Q \rightarrow 1$. It is interesting to observe that in this limit

$$G \rightarrow -4\pi \cdot \delta(k)/k,$$

referred to as the phase-shift approximation [19] with no dependence on Λ . (Note the limit gives δ NOT $\tan\delta$). But it is important here that this requires a complete (all order) ladder-summation to be made as in eq. (6).

One might expect the phase-shift approximation to be useful for a low-density neutron-gas. It was however already found by Sood and Moszkowski [2] that a proper treatment of the Pauli-blocking at low density, ($0.1 < k_f < 0.5 fm^{-1}$) and zero temperature reduces the potential energy/neutron by a factor of $\sim 1/2$ relative to this approximation. The dimensionless quantity to consider is in fact $k_f \cdot a_s$. With $a_s \sim 20 fm$ for the neutrons this would require $k_f \ll .05$, i.e. an extremely low density for the phase-shift approximation to be valid.²

A first order approximation $G(k) \sim \langle k|V_\Lambda|k \rangle$ would on the other hand be valid only for complete blocking, or for a weak potential in which case $G \sim V \sim \delta/k$. (With Λ sufficiently small, i.e. $V_{low k}$ weak enough, one may hope to reach this limit.)

Blocking also increases with density so that a first order approximation may become useful in this case. This is consistent with the findings by Moszkowski and Scott.[20] They show the second order contribution from their long-ranged part to decrease with increasing density. The long-ranged part in their separation-method corresponds to our low-momentum interaction with $\Lambda \sim 2 - 3 fm^{-1}$ and it also relates to $V_{low k}$. [21] Numerical agreement between the Moszkowski-Scott method and $V_{low k}$ was shown in ref. [17].

It was already emphasised above that eq. (6) for the G -matrix is a ladder summation to all orders of the bare interaction. Below we shall also do a calculation to second order using $G \rightarrow G^{(2)}$ with

$$\langle k|G^{(2)}|(P, \omega)|p \rangle = v(k)v(p)(1 - I_G(P, \omega)) \quad (8)$$

Note that with a separable interaction there is no difference in computing effort between second and all orders.

Calculations will also be shown below to first order i.e. with

$$\langle k|G^{(1)}|(P, \omega)|p \rangle = v(k)v(p) \quad (9)$$

All Brueckner calculations were done neglecting the dispersion correction, i.e. without self-energy insertions in particle- and in hole-lines. This approximation is justified by the results of ref. [16] showing this correction to be small in the 1S_0 channel. (See also ref.[3].) But it is not part of the Green's function calculations. There, the calculation of the T -matrix involve integrations over the spectral-functions that by their definition implicitly contain the self-energies.

In the Brueckner case a combination of eqs (6) and (4) gives [15, 14].

$$G(k, P) = -\frac{v^2(k; \Lambda)}{I_{GK}(k, P)} \quad (10)$$

with

$$I_{GK}(k, P) = \frac{1}{(2\pi)^3} \int_0^{2k_f} v^2(k'; \Lambda) \frac{Q(k', P) - \mathcal{P}}{k^2 - k'^2} k'^2 dk' + \frac{kv^2(k; \Lambda)}{\tan \delta(k)} \quad (11)$$

Eqs (10, 11) have the advantage over eqs (6, 7) in that the integrand in eq. (11) is zero for $k' > 2k_f$ because the factor $Q(k', P) - \mathcal{P}$ is then equal to zero. Although the two sets of equations are numerically identical the

²I thank Prof. Nai Kwong for helpful discussions relating to this observation.

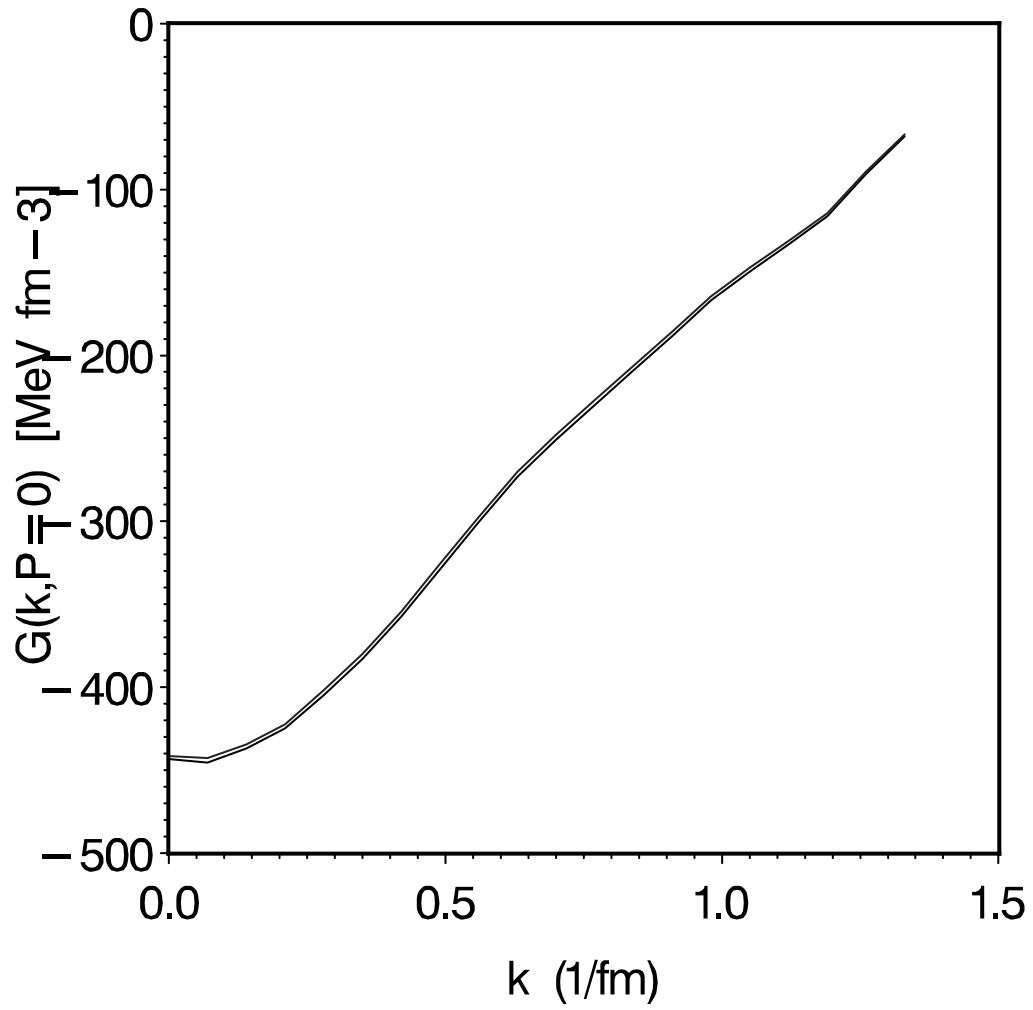


Figure 2: $G(k, P = 0)$ calculated from the two potentials of Fig. 1. There is complete overlap of the two curves. The fermi-momentum is here $k_f = 1.0 \text{fm}^{-1}$.

latter set simplifies the computing greatly. The high momentum component of the interaction is eliminated. This new equation also shows that G is independent of scaling $v(k; \Lambda)$ with a constant factor. Fig. 1 shows this to be approximately true and it at least partly explains the result shown by Fig. 2, the independence of Λ . Note however that the above eqs (10) and (11) are obtained only if assuming the neglect of the dispersion correction mentioned above.

Apart from this modified expression, used here at zero temperature the Brueckner calculation of the energy proceeds as described repeatedly in the literature.

At finite temperatures the Pauli-blocking is modified as shown by Bloch and DeDomicis. Only two-body interactions were included here. Obviously, 3-body etc and higher order graphs become important with increasing density.

3 Green's Function Method

Expressions and discussions relating to the Green's function equations for the in-medium T-matrix, self-energies and total energy of a fermion-system can be found in numerous publications. [23, 25, 26, 27] Only a summary of equations used in this work are shown here.

Like in the previous section the formalism is only shown for a rank one potential with the modifications for the rank 2 done as in ref.[11].

With the separable two-body interaction defined above the in medium T -matrix is given by (the dependence on Λ is suppressed but is implicit)

$$\langle k|T|(P, \omega)|p \rangle = \frac{v(k)v(p)}{1 - I(P, \omega)} \quad (12)$$

where P is the center of mass momentum and

$$I(P, \omega) = \int \frac{k^2 v^2(k) dk}{(2\pi)^3} \int d\cos(\theta) \int \frac{d\omega'}{2\pi} \int \frac{d\omega''}{2\pi} \frac{S(p_1, \omega' - \omega'') S(p_2, \omega'') (1 - f(\omega' - \omega'') - f(\omega''))}{\omega - \omega' + i\eta}.$$

where

$$p_{1,2} = \frac{P^2}{4} + k^2 \pm Pk\cos(\theta).$$

The imaginary part of the selfenergy is given by

$$Im\Sigma(p, \omega) = \frac{3}{8\pi} \int \frac{d\omega'}{2\pi} \int \frac{d\mathbf{k}}{(2\pi)^3} \langle \frac{\mathbf{p} - \mathbf{k}}{2} | ImT(|\mathbf{p} + \mathbf{k}|, \omega + \omega') | \frac{\mathbf{p} - \mathbf{k}}{2} \rangle S(k, \omega') (f(\omega') + b(\omega + \omega')).$$

where $b(\omega)$ is the Bose function. The real part $Re\Sigma$ is obtained by the usual dispersion relation and the HF-term is added.

With the self-energies given, the spectral function is calculated and a new T-matrix is obtained. The system of equations are iterated until convergence. At each iteration the chemical potential is calculated from the nucleon density. The correlated distribution function differs from the fermi-distribution and is given by

$$n(p) = \frac{1}{2\pi} \int f(\omega) S(\omega, p) d\omega \quad (13)$$

and the removal energy is

$$r(p) = \frac{1}{2\pi n(p)} \int \omega f(\omega) S(\omega, p) d\omega \quad (14)$$

The total energy is given by

$$E = \frac{1}{(2\pi)^3} \int d\mathbf{p} [p^2/2m - r(p)] n(p) \quad (15)$$

4 Numerical Results

4.1 Energy-Density Results;¹ S_0 .

Fig. 3 shows the energy per particle of the neutron-gas as a function of density at temperatures 0, 3, 4, 6 and 10 MeV. The full lines are from the Brueckner-Bloch-DeDomicis calculations. The crosses are from the Green's

function calculations. The short full lines are virial results obtained from the work of Horowitz and Schwenk [10].

The Brueckner calculations were done using standard methods with the cut-off $\Lambda = 3fm^{-1}$ and/or $\Lambda = 6fm^{-1}$ at the highest density. Increasing Λ did not change the results while a decrease of Λ showed noticeable differences as shown below in section 4.2. It can be remarked that the Brueckner calculations with the separable potential and inverse scattering are extremely simple and flexible. Any set of inputted phase-shift data provides an output of binding energy in seconds. Dependences on Λ are easily explored. The momentum-mesh was $0.01fm^{-1}$.

For the Green's function calculations, the set of equations (in medium T-matrix, self-energy Σ 's and spectral functions) were iterated until the total energy and chemical potential were stationary. This could require anywhere from 5 to 20 iterations depending on the input spectral functions. The in medium T-matrix was calculated with the separable potential as defined above and with the momentum cut-off kept constant at $\Lambda = 3fm^{-1}$. The ω -integrations were typically from -250 to $+250MeV$ with a mesh of $\sim 1MeV$.

The Green's function calculations are quite lengthy compared with the Brueckner calculations. They require a factor of thousands more computer-time. Although the equations (and the calculations) are rather different in the two cases, the results are surprisingly similar. This seems to agree (qualitatively) with zero-temperature results of other authors. [25, 27] A bonus is that the spectral functions contain more information on one particle properties such as distribution functions and removal energies. Using Thouless criterion[22] allows a determination of the BCS critical temperature. This was not investigated in detail but it was determined that $T_c \sim 3MeV$ at $n \sim 0.1fm^{-3}$. The spectral functions approach a quasi-particle limit at low temperatures and low density (See Fig. 9 below) and the energy-integrations then become numerically difficult. This can be resolved by resorting to the Extended Quasiparticle Approximation (EQP)[23, 24] or a similar method used by Bózek [26]. This was not done here as the Brueckner-Bloch-Domicis method appeared adequate for the present and also numerically so much easier.

4.2 Λ -dependence and low-order expansion; 1S_0

The dependence on the cut-off in momentum-space was discussed above. Here we show numerical results both for the complete Brueckner ladder summation, eq. (6), as well as for the second and first order expansions, eqs (8) and (9).

Fig. 4 shows the energy per particle at $T = 6MeV$ with the full G -matrix, eq. (6). Calculations were done for $\Lambda = 2, 3, 6$ and $8fm^{-1}$ with the Figure showing all results converging at the lowest densities. At higher densities the $\Lambda = 2$ curve is appreciably higher while for $\Lambda \geq 3$ one sees convergence.

Fig. 5 shows second order results, using eq. (8). They differ appreciably from the full G -matrix calculations as does the first order results shown in Fig. 6. The preferred Λ showing the best over-all agreement with the full G -matrix is $\Lambda \sim 2.5$ for $G^{(1)}$ and $\Lambda \sim 3$ for $G^{(2)}$. Comparing Fig. 4 with Fig. 5 one sees almost perfect agreement between the second order and full G -matrix results both for $\Lambda = 2$ and $3fm^{-1}$. Comparison with the first order results of Fig. 6 shows also good agreement there for $\Lambda = 2$ but less so for $\Lambda = 3fm^{-1}$. The force weakens if Λ decreases so that higher order terms then of course become less important. This is in qualitative agreement with the renormalisation results leading to $V_{low k}$. [4]

But only the full G -matrix result is capable of showing agreement with the virial expansion, at low density.

4.3 Energy-Density;including $L \leq 7$

Only the 1S_0 -states were included in the results presented above. At zero temperature that is sufficient for densities $\rho \leq 0.03fm^{-3}$.(see e.g.ref.[5]). At higher temperatures even the zero density virial expansion gets contribution from the higher partial waves [10] and 3N-forces are increasingly important with density and temperature increases. Fig.7 shows results including all partial waves $L \leq 7$. Comparison with Fig. 3 shows the decrease in energy from higher partial waves increasing with density while it is known that the contribution from 3N forces is repulsive and also increasing with density with the two effects partially cancelling each other. Comparison with Fig. 3 also confirms the statement made above regarding the contribution of higher partial waves to the virial expansion. Fig.7 also shows the Λ -dependence to increase with temperature.

The $T = 0$ result for $\Lambda = 2.5fm^{-1}$ agrees well with the NN-only results shown in refs[4, 28].

Second order calculations were also done for $\Lambda = 2.5$ with almost perfect agreement with the full Brueckner as is to be expected from the results shown in section 4.2.

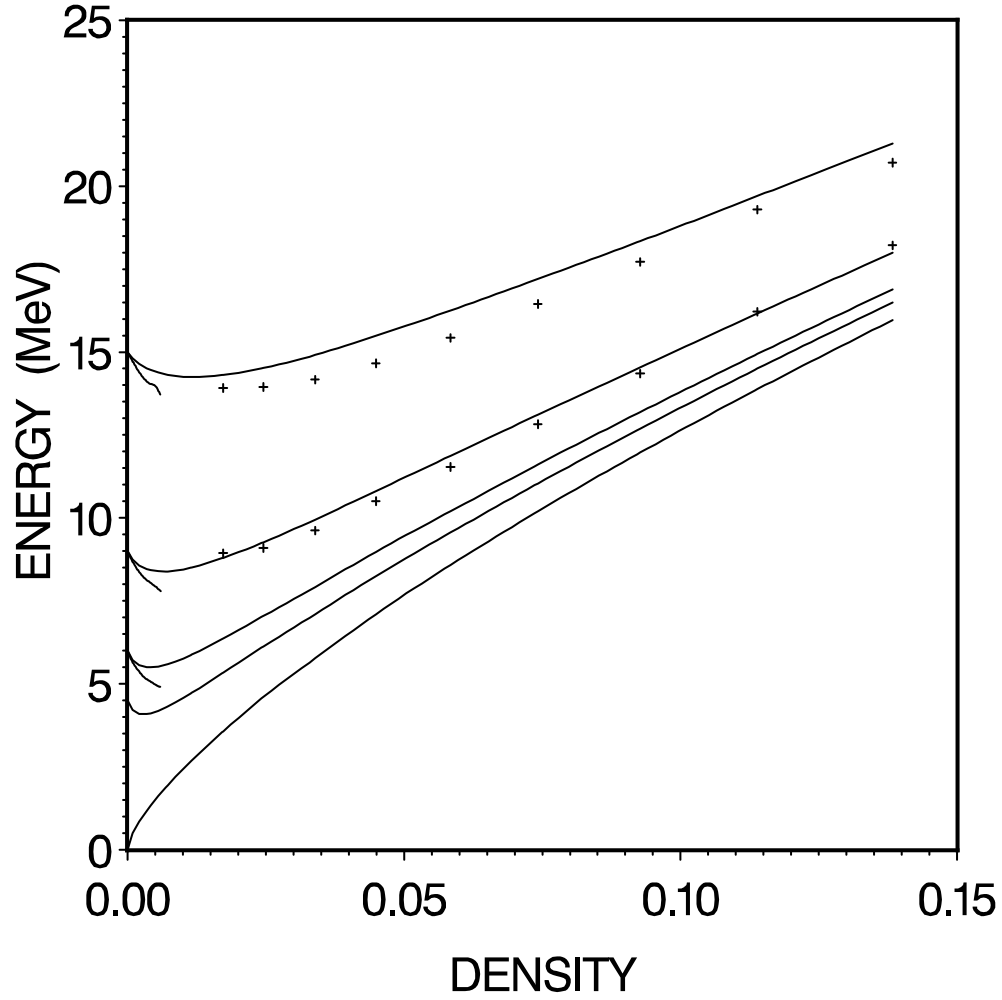


Figure 3: The solid lines show the energy at zero, 0, 3, 4, 6 and 10 MeV temperatures respectively from Brueckner ladder summations. The crosses are from Green's function calculations with selfconsistent spectral functions and with in-medium T -matrix ladders to all orders defined by eq. (12). Only 1S_0 -states included here. The short lines are low-density virial results from ref.[10].

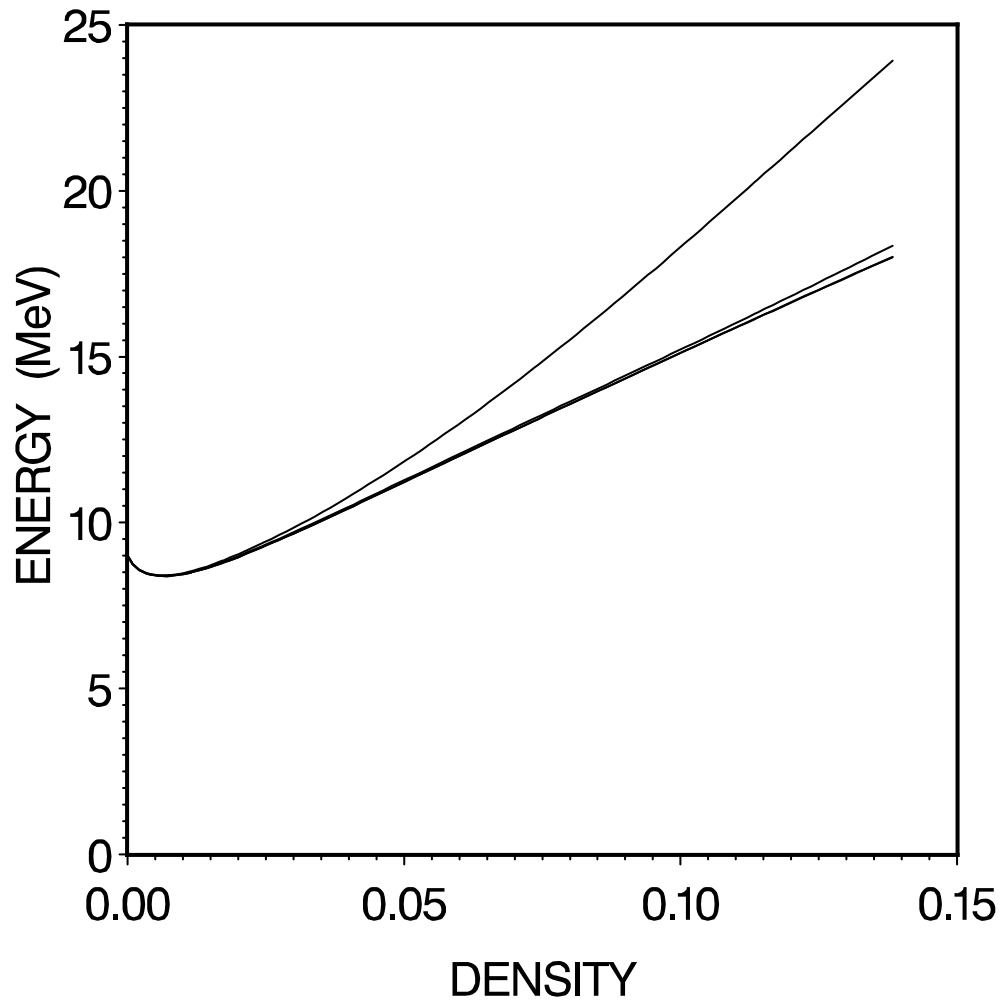


Figure 4: Shown are full G -matrix results, eq.(6), at $T = 6MeV$. The uppermost curve is for $\Lambda = 2fm^{-1}$, followed by $\Lambda = 3, 6$ and $8fm^{-1}$, the latter completely overlapping. 1S_0 -states only.

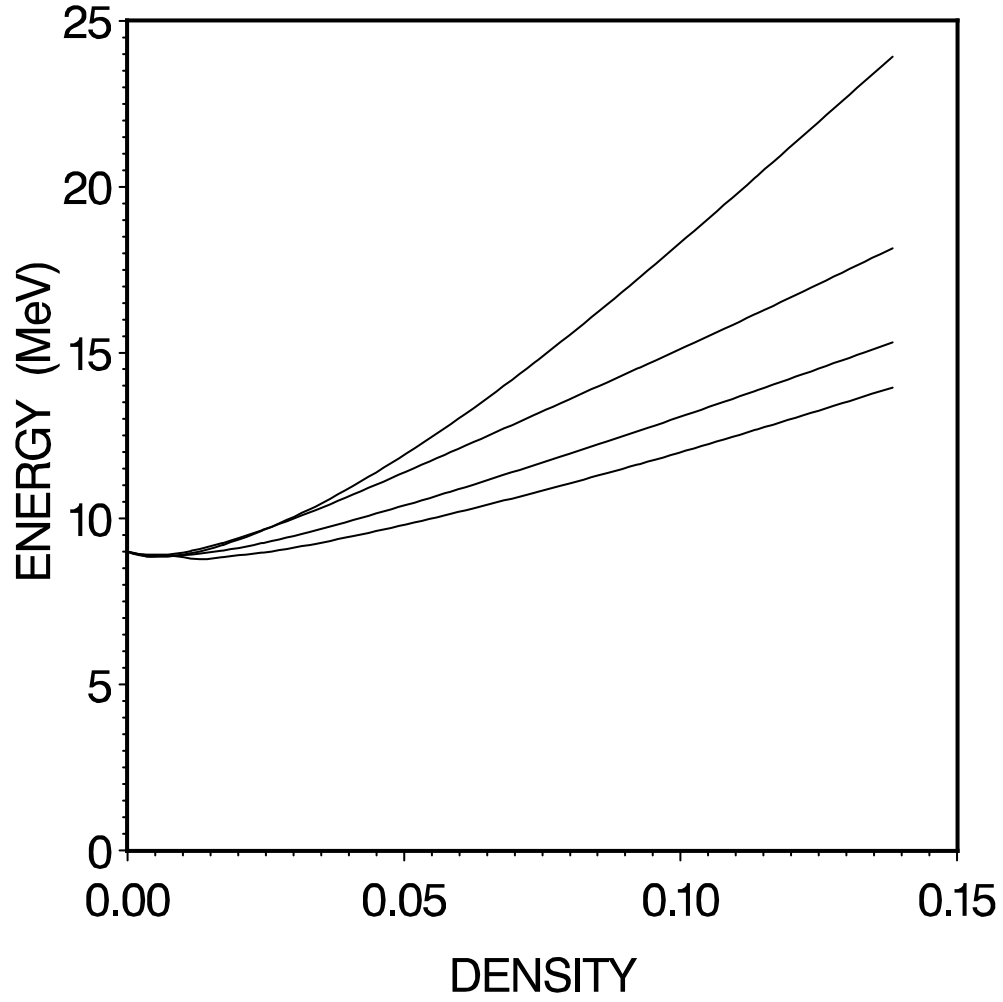


Figure 5: Shown are second order results eq.(8) at $T = 6MeV$. The uppermost curve is for $\Lambda = 2fm^{-1}$, followed by $\Lambda = 3, 6$ and $8fm^{-1}$. 1S_0 -states only.

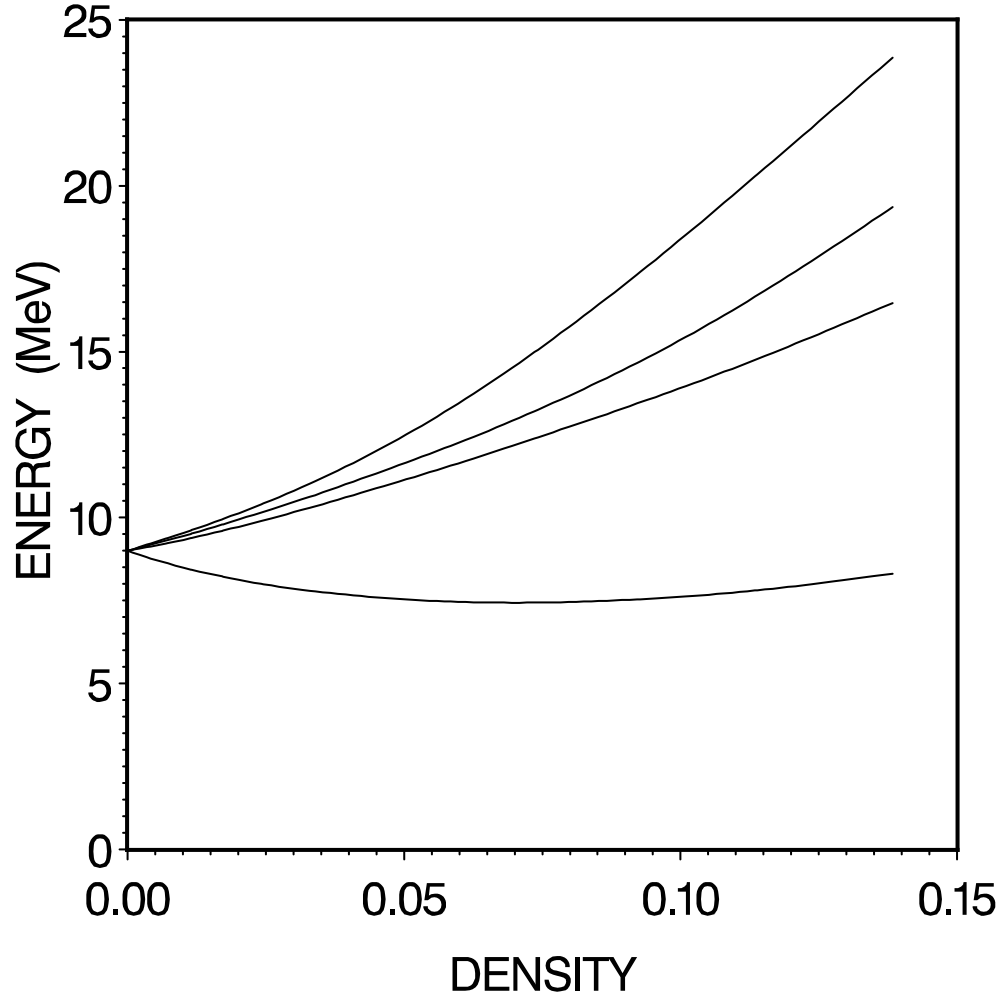


Figure 6: Shown are first order calculations eq.(9) at $T = 6MeV$. The uppermost curve is for $\Lambda = 2fm^{-1}$, followed by $\Lambda = 2.5, 3$ and $6fm^{-1}$. Note that the $\Lambda = 8$ curve is not shown. It would be much below the others. 1S_0 -states only.

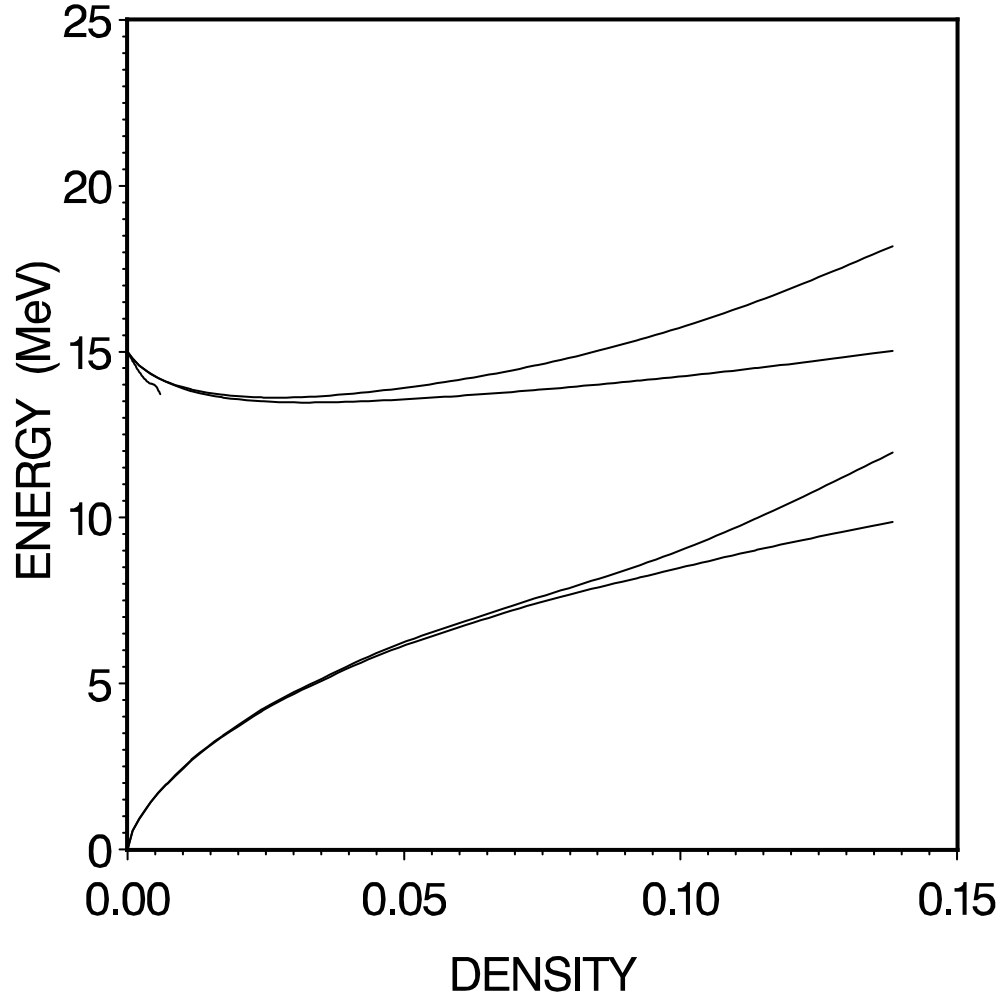


Figure 7: Energy as a function of density including all tw0-body states with $L \leq 7$. The two top curves are for $T = 10MeV$ with $\Lambda = 2.5fm^{-1}$ (upper curve) and $\Lambda = 5fm^{-1}$ respectively. The two lower curves are for $T = 0$ with the same values of Λ . The short line at $T = 10MeV$ is the virial expansion.

4.4 Spectral Functions etc

The output from Green's function calculations give a more detailed information about the many-body system than the corresponding Brueckner quasi-particle calculations. The additional information is contained in the spectral functions. Fig. 3 shows however that the quantity of interest here, the energy per particle as a function of density, is practically the same from the Brueckner as from the Green's calculations. The Green's function calculations are however computationally much more demanding, in particular at low density and low temperature where the quasiparticle picture dominates. The figures 8 and 9 both show spectral functions at a temperature $T = 10MeV$ but the first is at a high density while the second is at a low density. One may note that these spectral functions for the neutron-gas where the two-body interactions are only in the 1S_0 channel are rather different from those also including the 3S_1 states with stronger correlations.

5 Summary

The energy-density relation for neutron matter at densities ranging from zero to $\sim 0.14fm^{-3}$ and at temperatures ranging from zero to $10MeV$ have been computed. Two-body interactions were obtained from the free scattering phase-shifts by inverse scattering with momentum-cut-offs of $\Lambda = 2 \rightarrow 8fm^{-1}$. Three-body interactions were not included. The many-body calculations were made using Brueckner's technique extended to finite temperature by Bloch and DeDominicis. Insertions in hole- and particle-lines, i.e. dispersion corrections were neglected in this exploratory study as they are small for the states and densities considered here. They should of course be included in a "precision" calculation.

The free scattering interaction is in general Λ -dependent as illustrated in Fig.1 while the in-medium Brueckner G-matrix in Fig. 2 shows less or no dependence. This was discussed and partly explained above in section 2. Fig. 4 shows however that when calculating the total energy there is a significant difference between the $\Lambda = 2$ result and the $\Lambda \geq 3fm^{-1}$ results. But there is a nice convergence with increased Λ .

Our second order result is noticeably Λ -dependent although less so than the first order with no sign of convergence in any case and with considerable difference from the Brueckner results. The value of Λ with the best overall agreement with the Brueckner results is $\sim 2.5fm^{-1}$, which seems to agree with the $V_{low k}$ findings. It was also confirmed that for such a small value of Λ second order and Brueckner agree closely except, as remarked below, at low density..

We note that there is also a close agreement with Schwenk and Pethick. [5] for $T = 0$.

It was found, as did Tolos et al[4] that the higher order terms (in V) are necessary to correctly obtain the virial limits at finite temperatures associated with the energy minima in Fig. 3. In fact, it was found that the full Brueckner summation was desirable. But only 1S_0 states are included in this figure. Horowitz and Schwenk[10] find that the virial coefficient b_2 increases if higher partial waves are also included, thus further enhancing the minima. This increase in b_2 becomes larger with increased temperature (Table 1. of ref.[10]) and is about 20% at the highest temperature $T = 10MeV$ in our Fig. 3. The virial corrections shown in this figure are extracted from ref.[10] and include all partial waves. The importance of the higher partial waves in this case is in (qualitative) agreement with Fig.7. This is quite different from the situation at $T = 0$ as shown comparing Figs 7 and 3. The 1S_0 clearly dominates at low temperature and density.

Comparisons of the Brueckner results with Green's function results were made at $T = 6$ and $10MeV$ and an agreement within numerical uncertainties was seen.

A comparison between Brueckner and Green's function calculations for the neutron gas at zero temperature was done by Bózek et al[25]. These authors found agreement between the two methods for the densities considered here and their results also agree with the present work. At higher densities they found the Green's function results much more repulsive than the Brueckner.

The separable interaction used here may be considered phenomenological. It fits experimental on-shell scattering data. Off-shell data are not available. As illustrated in ref. [11] it does reproduce the half-off-shell data of the meson theoretically derived Bonn-potentials. As such it may be considered "realistic" for the 1S_0 -state. The separable nature of this interaction is supported by the large scattering length associated with the nearly bound state in the 1S_0 channel.[12] Further comparison with the Bonn-potentials for other states was found in ref.[11], an exception being the 3P_1 -state, requiring in this case that the rank of the potential be increased.

The 3N forces were not considered in the present work. They are important and should of course be included in the determination of the EOS, but are also less well determined than the 2N forces. A main purpose of the present study was to shed some light on the dependence on momentum cut-offs and to show that separable potentials derived for inverse scattering are useful for such a study.

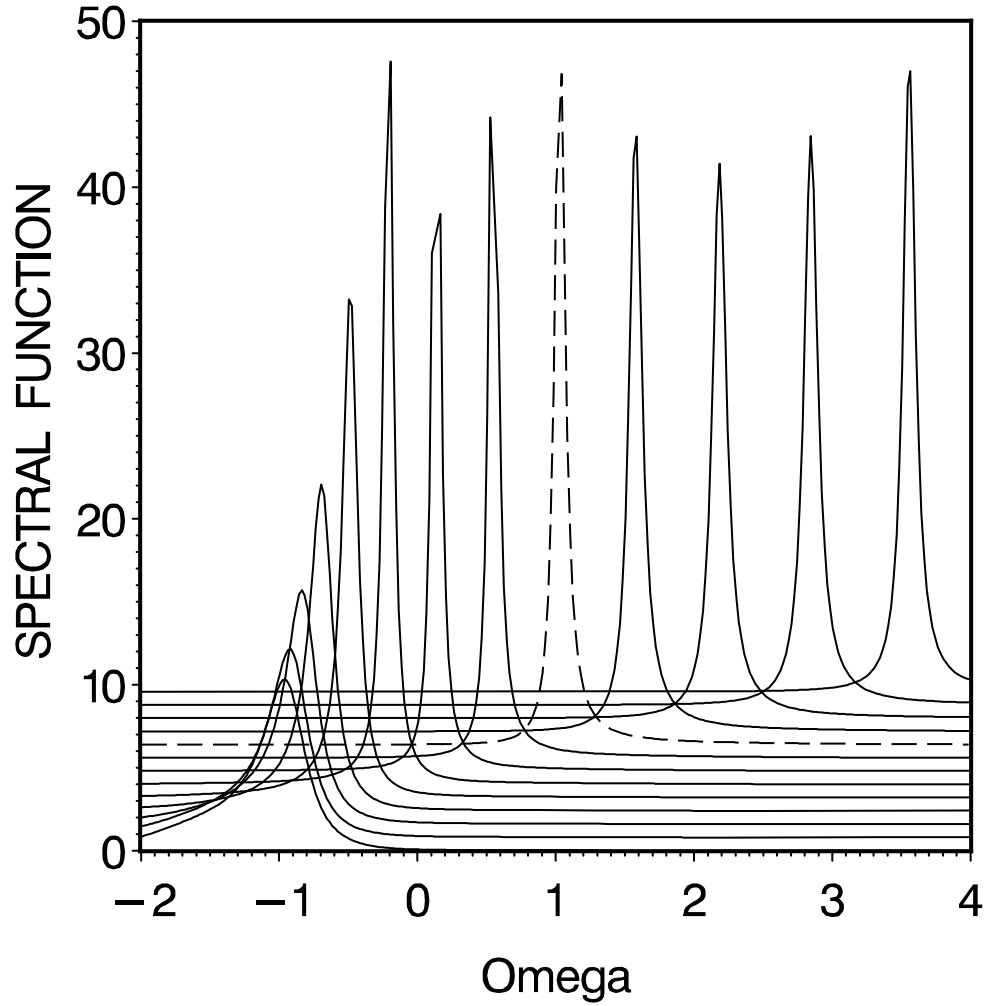


Figure 8: Spectral functions $S(p, \omega)$ at $T = 10 \text{ MeV}$ temperature and a density of 0.11 fm^{-3} . The energy ($\omega - \mu = \text{Omega}$) is in units of \hbar^2/m . (μ is chemical potential). The momenta are offset and range from $p = 0$ to the cut-off $\Lambda = 3 \text{ fm}^{-1}$. The broken curve is at the fermi-surface. Compare this with Fig. 9 which is for a lower density. 1S_0 -states only.

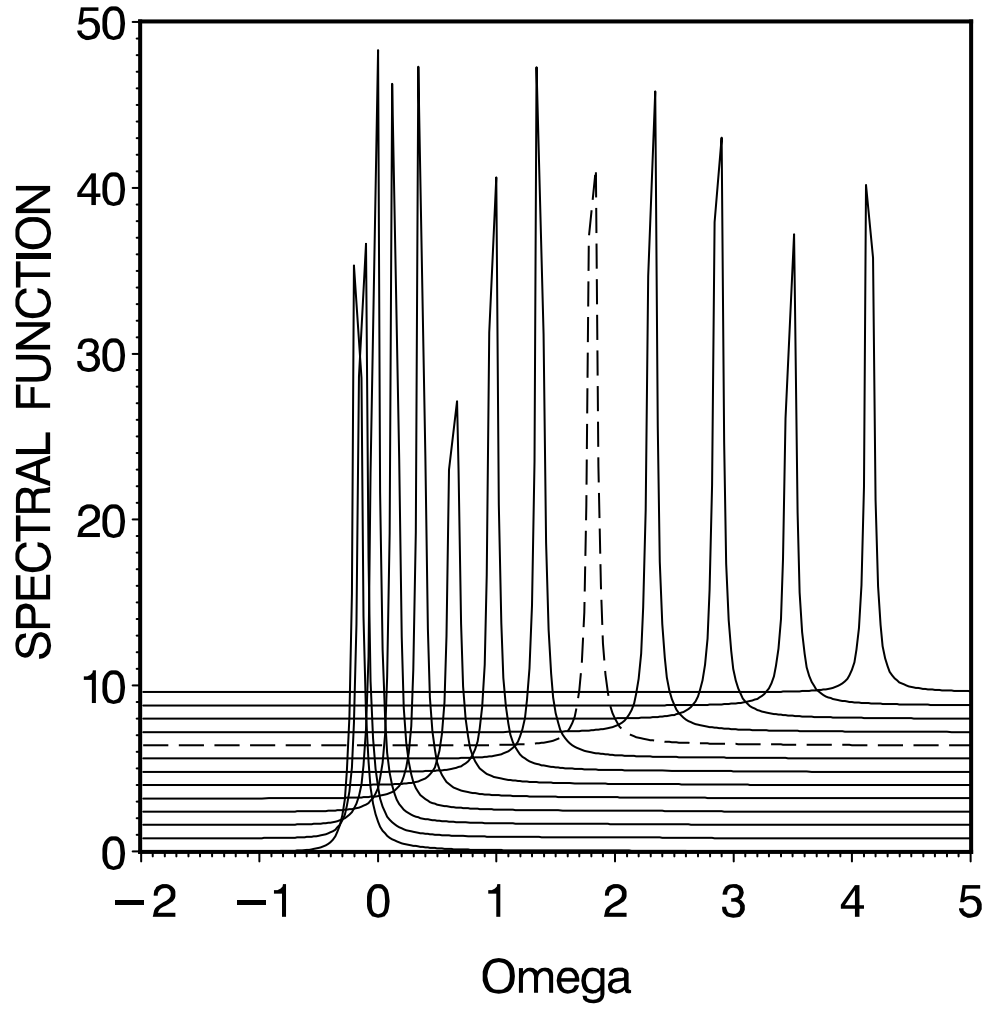


Figure 9: Similar to Fig. 8 but at a density of $0.017 fm^3$. Notice the sharply peaked functions indicating the closeness to a quasi-particle limit. This decreases the accuracy of the ω -integrations and requires special treatment. 1S_0 -states only.

References

- [1] C. Bloch and C. DeDomicis Nucl. Phys. **7** (1958) 459; **10** (1959) 509; **10** (1959) 459.
- [2] P.C. Sood and S.A. Moszkowski Nucl. Phys. **21** (1960) 582.
- [3] M. Baldo and C. Maieron nucl-th/0712.2662; Phys. Rev. C **77** (2008) 015801.
- [4] L. Tolos, B. Friman and A.Schwenk nucl-th/0611070;nucl-th/0711.3613.
- [5] A. Schwenk and C.J. Pethick Phys. Rev. Lett. **95** (2005) 160401.
- [6] Jérôme Margueron, Isaac Vidaña and Ignazio Bombaci Phys. Rev. C **68** (2003) 055806.
- [7] E. Kohn and J.M.Luttinger Phys. Rev. **118** (1960) 41.
- [8] J.M.Luttinger and J.C. Ward Phys. Rev. **118** (1960) 1417.
- [9] M. Baldo and L.S. Ferreira, Phys. Rev. **59** (1998) 682.
- [10] C.J. Horowitz and A. Schwenk, Phys.Lett. B **638** (2006) 153.
- [11] N.H. Kwong and H.S. Köhler, Phys. Rev. C **55** (1997) 1650.
- [12] G.E. Brown and A.D. Jackson "The nucleon-Nucleon Interaction", North-Holland (1976)
- [13] R. A. Arndt, "Interactive Dial-in Program SAID".
- [14] H.S. Köhler , nucl-th/0801.1123.
- [15] H.S. Köhler , nucl-th/0705.0944.
- [16] H.S. Köhler and S.A. Moszkowski, nucl-th/0703093.
- [17] H.S. Köhler , nucl-th/0511030.
- [18] M. Bolsterli and J. MacKenzie, Physics (Long Island City,NY) **2** 1965 141.
- [19] W.B. Riesenfeld and K.M. Watson, Phys. Rev. **104** (1956) 492.
- [20] S.A. Moszkowski and B.L. Scott Ann. of Phys. **11** (1960) 65.
- [21] J.W. Holt and G.E. Brown, nucl-th/0408047.
- [22] D.J. Thouless, Ann. of Phys. **10** (1960) 553.
- [23] H.S. Köhler and Rudi Malfliet, Phys. Rev. C **48** (1993) 1034.
- [24] P. Lipavský, K.Morawetz and V. Špička, Annales de Physique **26** (2001) 1.
- [25] P. Bózek and P. Czerski Phys. Rev. C **68** (2002) 027301.
- [26] P. Bózek, Phys. Rev. C **65** (2002) 054306.
- [27] T. Frick and H. Müether, Phys. Rev. C **68** (2003) 034310.
- [28] A. Schwenk,B. Friman and G.E. Brown, Nucl. Phys. **A713** (2003) 191.